

Contents lists available at [SciVerse ScienceDirect](http://www.sciencedirect.com)

Quaternary Geochronology

journal homepage: www.elsevier.com/locate/quageo

Research paper

Ages of Liangshan Paleolithic sites in Hanzhong Basin, central China

Xuefeng Sun^{a,*}, Huayun Lu^a, Shejiang Wang^b, Shuangwen Yi^a

^aSchool of Geographic and Oceanographic Sciences, The MOE Key Lab of Coast and Island Development, Nanjing University, No. 22, Hankou Road, 210093 Nanjing, China

^bJoint Laboratory of Human Evolution and Archaeometry, Institute of Vertebrate Paleontology and Paleoanthropology, Chinese Academy of Sciences, Beijing 100044, China

ARTICLE INFO

Article history:

Received 12 October 2011

Received in revised form

11 April 2012

Accepted 12 April 2012

Available online xxx

Keywords:

TT-OSL dating

Hanzhong Basin

Paleolithic site

Loess

Environmental change

ABSTRACT

Thermally transferred optically stimulated luminescence (TT-OSL) dating extends the age range beyond current limits of OSL dating in Chinese loess. In this study, we use a single-aliquot regenerative-dose procedure for TT-OSL protocol to date Yaochangwan and Hejialiang localities of loess-covered Liangshan Paleolithic sites in Hanzhong Basin, which is an important area for the study of Paleolithic industries during the middle Pleistocene in central China. The results suggest that buried culture layer at the Hejialiang locality is correlated with the last interglacial paleosol S1 in Chinese Loess Plateau, it is dated at 86.3 ± 6.4 ka. The Yaochangwan locality spans from approximate 600–100 ka and correlates with S5–S1 in the typical Chinese loess–paleosol sequences, respectively. These ages suggest that hominins already occupied the Hanzhong Basin since approximately 600 ka ago.

© 2012 Elsevier B.V. All rights reserved.

1. Introduction

The Hanzhong Basin is located to southern margin of Qinling Mountains in central China, which is conventionally regarded as boundary between the southern and northern climatic zones of China. Previous studies suggested that this region represents the transitional zone between predominantly pebble-core Paleolithic industry in the south and small core-retouched flake tools industry in the north during the Middle Pleistocene (Yan, 1980, 1981; The Archaeological Team of Shaanxi Archaeological Institute, 1985, 1988; Huang and Qi, 1987; Tang and Zong, 1987; Wang, 2000, 2008). In this basin, more than 1000 artifacts, including hand-axes, have been collected and excavated (Huang and Qi, 1987; The Archaeological Team of Shaanxi Archaeological Institute, 1985, 1988; Lu et al., 2006). Unfortunately, these artifacts have never been well dated and their ages are still unknown.

Since these Paleolithic artifacts were found in loess or paleosol deposits, which can be well dated. Therefore, by dating the loess the age of these artifacts can be obtained, assuming contemporaneous deposition of loess and artifacts. As a result of the limitations of dating techniques or material, the ages of most middle Pleistocene archaeological sites in China, in particular those younger than the Brunhes/Matuyama boundary (0.78 Ma), are not well

established. In this study, we use thermally transferred optically stimulated luminescence (TT-OSL) dating method, which has shown promise for dating middle Pleistocene aeolian deposits (Wang et al., 2006a, 2006b, 2007; Stevens et al., 2009; Sun et al., 2010).

The first investigations of TT-OSL signal were carried out by Smith et al. (1986) and Aitken and Smith (1988). Wang et al. (2006a, 2006b, 2007) used TT-OSL for dating of quartz. But a number of problems were reported with the use of this sequence, and several modifications to the SAR TT-OSL protocol were proposed (Tsukamoto et al., 2008; Porat et al., 2009; Stevens et al., 2009; Adamiec et al., 2010). Stevens et al. (2009) showed a protocol (Table 1) applicable to a variety of coarse and fine-grained samples in Chinese loess. In this protocol, reproducible dose response curves that saturate at high doses and pass through zero within errors were produced. Furthermore, signal growth was observed up to at least 12 kGy and known doses of up to 0.56–1.2 kGy could be recovered (Stevens et al., 2009). Therefore, this TT-OSL protocol may be useful to extend the age range beyond current limits of OSL in the Hanzhong Basin.

2. New investigation

Previous investigations showed that the Hanzhong Paleolithic Industry is characterized by its assemblage of chopper-chopping tools, spheroids, hand-axes, and picks (Yan, 1980, 1981; The Archaeological Team of Shaanxi Archaeological Institute, 1985,

* Corresponding author.

E-mail address: xuefeng@nju.edu.cn (X. Sun).

Table 1
The SAR TT-OSL dating protocol (Stevens et al., 2009).

Dose	
Preheat (260 °C, 10 s)	
OSL (125 °C, 60 s)	
Preheat (260 °C, 10 s)	
TT-OSL (125 °C, 60 s) (L_x)	
OSL (280 °C, 400 s)	
Test dose	
Preheat (260 °C, 10 s)	
OSL (125 °C, 60 s)	
Preheat (260 °C, 10 s)	
TT-OSL (125 °C, 60 s) (T_x)	
OSL (290 °C, 400 s)	

1988; Huang and Qi, 1987; Tang and Zong, 1987). The Hanzhong lithic assemblage has close relationships with the lithic artifacts which unearthed from the Lantian Man site, the Luonan sites, the Yunxian Man site, and the Dingcun sites (Yan, 1980, 1981; The Archaeological Team of Shaanxi Archaeological Institute, 1985, 1988; Huang and Qi, 1987; Lu et al., 2006; Shaanxi Provincial Institute of Archaeology et al., 2007). These sites are all located very close to each other in or around the Qinling Mountains. The Hanzhong Paleolithic Industry is regarded as one of the earliest Paleolithic industries in the area.

Since 2009, we have conducted new field investigations in the Hanzhong Basin near the Liangshan Mountain area. In total, seven loess-covered Paleolithic localities have been investigated in detail (Beizhai, Nanzhai, Wangjiaxiang, Yaochangwan, Longgangsi, Hejialiang, and Yongyuancun), in addition, two of which, the Hejialiang and the Yongyuancun localities, were newly discovered. Three natural loess sections (Yutang, Tudimiao and Limingcun) were investigated in detail. More than 100 artifacts from the Hejialiang locality, including a hand-axe-like tool (Fig. 1b), and more than 30 artifacts from the Yongyuancun locality, have been collected. We have also collected more than 20 artifacts at the Yaochangwan locality, which is only approximately 2 km away from the Longgangsi locality, including a large cutting tool (Fig. 1a). Most artifacts were found on the surface close to the loess section. These artifacts were likely picked out and discarded by local farmers.

Fortunately, separate artifacts were found *in situ* at the bottom of the Yaochangwan and Hejialiang loess section (Fig. 2) in the summer of 2010. Furthermore, a number of artifacts have also been excavated from Longgangsi section in 1980s (Yan, 1980, 1981; The Archaeological Team of Shaanxi Archaeological Institute, 1985, 1988), which is in the same layer as in Yaochangwan section (Fig. 2). Therefore, dating the bottom of loess sediment at the base of the Hanshui River terraces is useful for understanding age of the Hanzhong hominids.

3. Geographical setting

The Hanzhong Basin is an intermountain depression, with an elevation of 500 m, through which the Hanshui River flows eastward into the Yangse River in Wuhan. Loess sediment, with thicknesses ranging from 1 to 20 m, was deposited on the Hanshui River terraces and many small tablelands in the Hanzhong Basin, which also contains distinct loess–paleosol alternations. There is a large difference in loess thickness between the Hanzhong Basin and the central Loess Plateau where the thickness can reach more than 100 m (Liu, 1985; Kukla and An, 1989; Lu et al., 1999, 2004).

Paleolithic remains are buried in the loess sediments from the first to third terrace of the Hanshui River. The Hejialiang, Yongyuancun, and Limingcun sections are situated on the first terrace with an elevation of 505–510 m at its base. The Beizhai, Nanzhai,

Wangjiaxiang, Yaochangwan, and Longgangsi sections are located on the second terrace with an elevation of 520–525 m at its base. The Yutang and Tudimiao sections on the third terrace are the highest sections, with an elevation of 540–545 m at the base (Fig. 2). The bases of these sections comprise of typical fluvial sand, pebbles, and cobbles derived from the Hanshui paleo-river channel (Fig. 2).

In this study, the Hejialiang section on the first terrace and the Yaochangwan section on the second terrace were sampled in detail, as they are the representative sections on the Hanshui River terraces. In the Hejialiang locality, there is a thin eolian deposit with thickness of 520 cm covering on the fluvial sand, pebbles, and cobbles. An *in situ* artifact was just found at the lower part of the only paleosol layer in Hejialiang section (Fig. 2). In the Yaochangwan locality, distinct loess and paleosol alternations are present on the second river terrace with a thickness of more than 1500 cm. From this loess–paleosol sequence, we identified five loess units and five paleosol complexes. Two *in situ* artifacts were found in the fifth paleosol layer at a depth of 1400 cm (Fig. 2).

4. Method

4.1. Sampling

Fieldwork at the Hejialiang and the Yaochangwan localities was carried out in August 2010 and May 2011, with two additional visits in 2009. We took two samples at Hejialiang section and five samples at Yaochangwan section for TT-OSL dating by inserting metal tubes in cleaned loess sections. Samples were preserved in black bags and sealed with waterproof tape. HJL-1 and HJL-2 were sampled at the upper and lower part of the unique paleosol layer from 180 cm to 370 cm depth, respectively, at the Hejialiang section on the first terrace (Fig. 2), and the depth of 370 cm is the position for separate artifact finding. At the Yaochangwan section on the second terrace, both YCW-1 and YCW-2 were sampled in the first paleosol unit at 180 cm and 310 cm depth, respectively, and YCW-3 was sampled in the next loess layer at 360 cm depth. YCW-4 and YCW-5 were sampled from the second paleosol unit at 410 cm and 460 cm depth, respectively (Fig. 6). Moreover, in January 2012 we collected an additional sample named YCW-6 in the artifact layer at the bottom of Yaochangwan section at 1400 cm depth.

Samples for proxy indexes of paleoenvironment variations were also taken in the Hejialiang and the Yaochangwan sections at an interval of 5 cm, yielding 104 and 308 bulk samples, respectively. These samples were then prepared for magnetic susceptibility measurement, and 30 cubic samples ($2 \times 2 \times 2 \text{ cm}^3$), with the north direction marked on the top face, were measured for paleomagnetic stratigraphy analysis.

4.2. Magnetostratigraphic analyses

The magnetic susceptibility of the Chinese loess–paleosol sequences is high in soils and low in loess units (Heller and Liu, 1984). Therefore, it is regarded as a good proxy of paleoclimatic changes (Liu and Ding, 1998). As a result, the measurement of magnetic susceptibility serves an important role in distinguishing the soil and loess layers in the loess sections of the Luonan Basin and Lushi Basin (Lu et al., 2007, 2011). The magnetic susceptibility of Hejialiang and Yaochangwan sections was measured with a Bartington MS-2 magnetic meter in the laboratory at Nanjing University, and the results are shown in Figs. 5 and 6.

Paleomagnetism was also evaluated. The oriented cube samples were systemically heated in a zero magnetic field, in a stepwise fashion to demagnetize secondary magnetism. The demagnetized samples were measured using the 2G superconductor magnetic

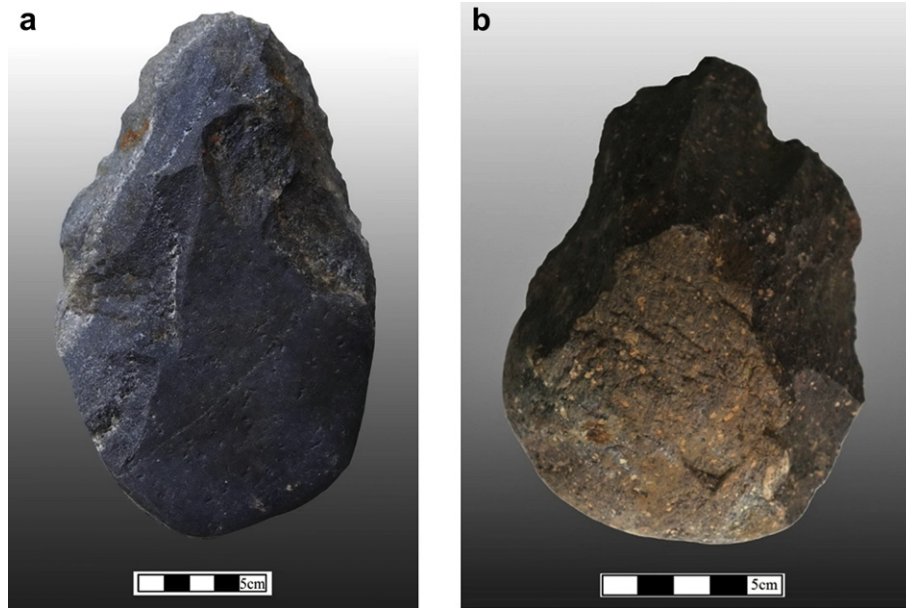


Fig. 1. (a) A representative stone artifact collected from the Yaochangwan locality. (b) A representative stone artifact collected at the Hejialiang locality.

meter in Nanjing University. The principal components direction was computed by a ‘least-squares fitting’ technique (Kirschvink, 1980). For the paleomagnetic stratigraphy analysis, the inclinations of all cubic samples are positive, so the Hejialiang and Yaochangwan loess–paleosol sequences were correlated with the Brunhes positive magnetic chron (N1). These results show that the loess deposits in both Hejialiang and Yaochangwan section are younger than the Brunhes/Matuyama (0.78 Ma) boundary (Cande and Kent, 1995).

4.3. SAR TT-OSL

4.3.1. Laboratory methods

The two ends of the samples that may have been exposed to daylight during sampling were removed in the laboratory under subdued red light and used for water content measurements and neutron activation analysis. The unexposed parts of the samples were prepared to extract pure quartz grains. The size fraction of 40–63 μm was chosen and extracted by wet sieving. The grains

were then treated with 10% HCl and 30% H_2O_2 to remove carbonates and organic matter, etched by 40% HF to remove feldspars, and sieved again. Quartz grains were mounted as a monolayer with a 5 mm spray mask on the 9.8 mm diameter aluminum disks using silicone spray oil. The purity of the isolated quartz was checked by IR stimulation, and no significant IRSL signal of the isolated quartz was detected.

All signals were measured on a Risø TL/OSL-DA-20C/D reader. Blue LED ($\lambda = 470 \pm 30 \text{ nm}$) stimulation sources were used. The OSL and TT-OSL signal was measured using a 9235QA photomultiplier tube and a 7 mm Hoya U340 glass filter (Bøtter-Jensen et al., 1999). All of the measurements were carried out in Luminescence Dating Laboratory of Nanjing University. For the 40–63 μm grains, an alpha efficiency (a-value) of 0.035 ± 0.02 (Rees-Jones, 1995; Lai et al., 2008) was used. Concentrations of U, Th, and K were obtained by neutron activation analysis (NAA). The average water content was 15% (Table 1). The cosmic dose was calculated using present-day burial depth (Prescott and Hutton, 1994).

4.3.2. D_e determination

In order to determine whether the test dose is appropriately monitoring sensitivity change, the relationship between the regeneration (L_x) and test dose (T_x) signals (Murray and Wintle, 2000) was examined by repeating identical regeneration and test dose measurements during the SAR TT-OSL sequence (Table 2) for five separate sets of 3 aliquots (15 in total) of sample YCW-4. Prior to the first cycle dosing, the sets of aliquots were bleached in different ways. The first set was bleached at room temperature using blue diodes twice for 300 s; the second set was bleached using sunlight (Nanjing, January) for one day; the third set was bleached using a solar simulator (SOL) for 3 h; the fourth set was bleached using a SOL for 215 h. The fifth set was bleached at room temperature using blue diodes twice for 300 s (identical to the first set) but was not given regeneration doses. The L_x against T_x relationship is consistent with a straight line that passes within 1σ of the origin, demonstrating an apparently accurate sensitivity correction (Fig. 3a). However, there are significant differences in the L_x/T_x values of the initial first cycle measurement between the aliquot sets, and when compared to L_x/T_x values from the second

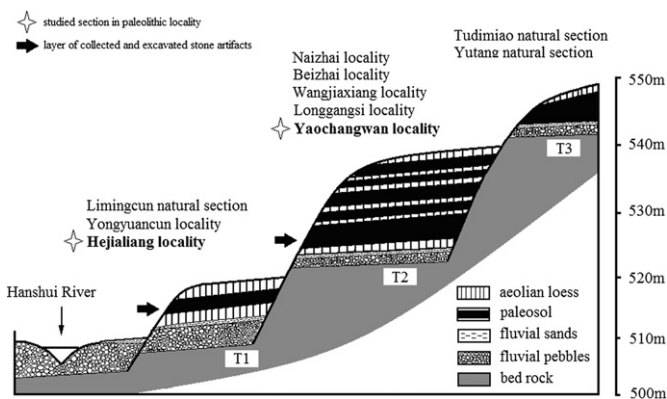


Fig. 2. Investigations of Paleolithic localities and natural loess sections at the Hanshui River terraces (from T1 to T3). The studied loess sections were at the Yaochangwan locality and the Hejialiang locality.

Table 2
Radioactive data, water content, equivalent dose, dose rate and the TT-OSL ages of the samples from the Hejialiang and Yaochangwan sections.

Sample no.	Depth (m)	U (ppm)	Th (ppm)	K (%)	Water content (%)	Dose rate (Gy/ka)	DE (Gy)	Age (ka)
HJL-1	1.8	2.50 ± 0.10	12.9 ± 0.37	2.36 ± 0.08	15	3.44 ± 0.21	256.8 ± 6.9	74.6 ± 5.0
HJL-2	3.8	2.79 ± 0.10	13.1 ± 0.37	2.49 ± 0.07	15	3.59 ± 0.22	310.0 ± 12.9	86.3 ± 6.4
YCW-1	1.8	2.77 ± 0.10	13.4 ± 0.38	2.31 ± 0.07	15	3.49 ± 0.22	314.2 ± 24.9	90.1 ± 9.1
YCW-2	3.1	2.65 ± 0.10	13.2 ± 0.37	2.02 ± 0.06	15	3.18 ± 0.21	377.8 ± 26.8	118.8 ± 11.3
YCW-3	3.6	2.82 ± 0.10	13.3 ± 0.37	2.03 ± 0.06	15	3.22 ± 0.21	500.1 ± 17.7	155.2 ± 11.4
YCW-4	4.1	3.01 ± 0.10	14.5 ± 0.40	2.16 ± 0.06	15	3.44 ± 0.22	553.9 ± 17.7	161.2 ± 11.7
YCW-5	4.6	3.21 ± 0.10	14.0 ± 0.39	1.90 ± 0.06	15	3.22 ± 0.22	555.8 ± 22.5	172.6 ± 13.7
YCW-6	14.0	3.05 ± 0.12	14.6 ± 0.41	2.04 ± 0.06	15	3.27 ± 0.22	506.0 ± 19.8	154.7 ± 12.2

cycle onwards. We propose that this indicates differences in the degree of bleaching and reinforces previous findings concerning the hard to bleach nature of the TT-OSL signal. The one-day sunlight bleach yields similar L_x/T_x changes between the first and second cycles to the reader bleaching described above (Fig. 3b and d). A 3 h SOL bleach gave slightly larger drops in L_x/T_x between the first and second cycles, indicating less efficient bleaching (Fig. 3c). However, when we extend the SOL bleach there is a considerable reduction in first cycle L_x/T_x values and no apparent drop to the second cycle L_x/T_x (Fig. 3e). This pattern is consistent with what would be expected if the first cycle L_x/T_x values were influenced by residual TT-OSL from the natural to differing degrees, dependent on bleaching intensity and duration. This is further reinforced by the finding that

when only reader bleaching is used, and no regeneration doses are given, the first cycle L_x/T_x is high, but falls to negligible values in the second cycle onwards (Fig. 3f). This is consistent with the presence of an initial signal prior to first measurement, but one which is entirely removed during measurement of the first cycle L_x/T_x . It is interesting to note that when bleached for 215 h in the solar simulator, the entire residual signal seems to be removed and L_x/T_x cycling is consistent across all measurement cycles. Therefore, we conclude that any sensitivity change during the measurement cycle is being monitored successfully.

After these tests, measurements of the SAR TT-OSL sequence were carried out. TT-OSL dose response curves of all the samples are similar (Fig. 4). The sensitivity change correction produced

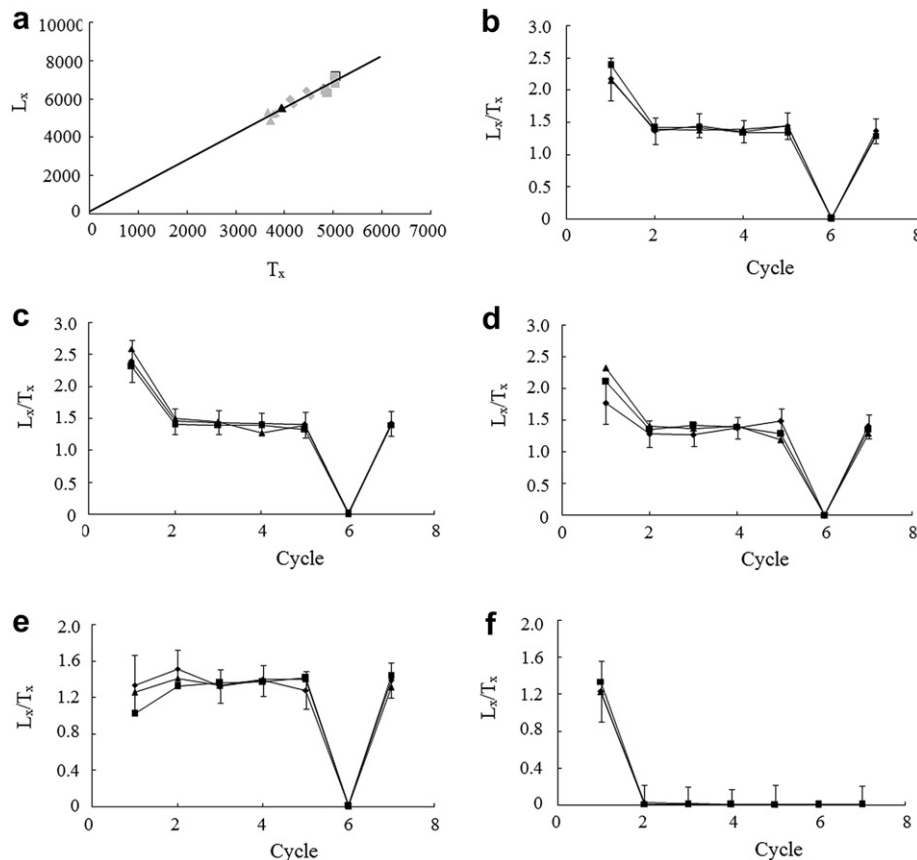


Fig. 3. (a) L_x against T_x after repeating identical doses between each cycle as part of the sequence in (Table 1) on three aliquots of YCW-4 ($L_x = 420$ Gy dose; $T_x = 280$ Gy dose) after initial bleaching at room temperature by blue diodes in a luminescence reader twice for 300 s. Natural cycles are shown by black symbols. (b) L_x/T_x against measurement cycle at a constant regeneration dose for three aliquots of YCW-4 (same data as in part a). The 1st cycle is the remaining natural (after laboratory bleaching as in a) + β and the sixth cycle is the zero dose point. (c), (d) and (e) L_x/T_x against measurement cycle at a constant regeneration dose for three aliquots of YCW-4 after separate bleaching treatments. (c) Bleached by sunlight for one day; (d) and (e) Bleached by solar simulator for 3 h and 215 h respectively. (f) L_x/T_x against measurement cycle without the application of regeneration dose after initial bleaching at room temperature by blue diodes in a luminescence reader twice for 300 s for three aliquots of YCW-4.

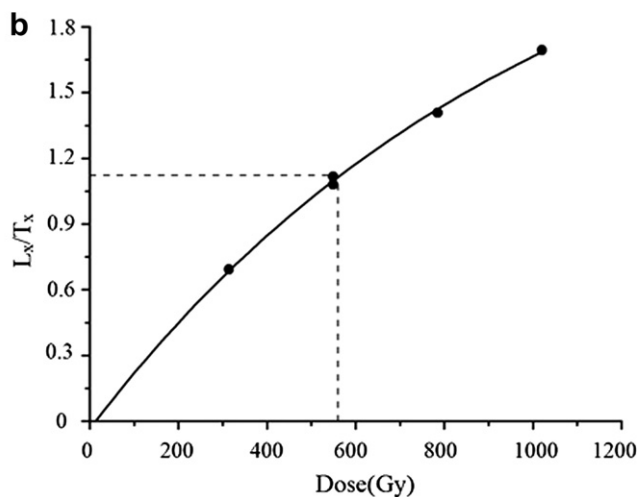
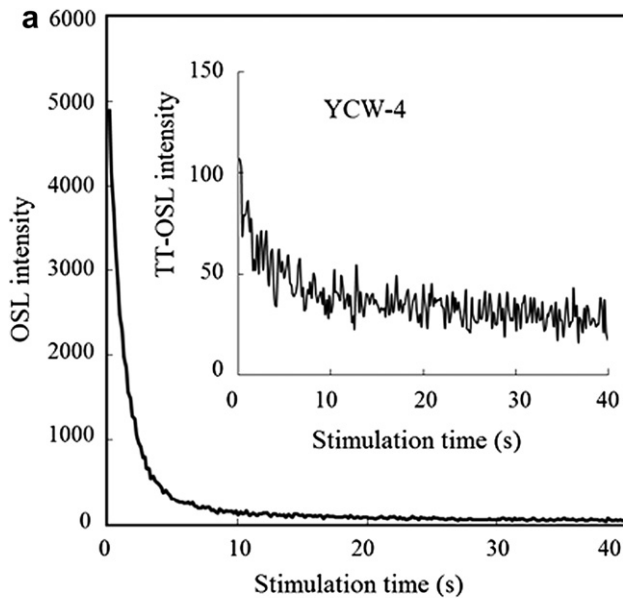


Fig. 4. (a) The natural OSL signal decay curve and the natural TT-OSL signal decay curve of the middle-sized quartz from the YCW-4 sample. (b) The average TT-OSL regenerated growth curves calculate from eight growth curves of YCW-4.

recycling ratios in the 0.90–1.10 range for HJL-1, HJL-2, and from YCW-1 to YCW-3, and in the 0.85–1.5 range for YCW-4 and YCW-5. The average recycling ratio of all the aliquots we used is 1.03 ± 0.01 . All dose response curves were fitted using linear, saturating-exponential or saturating-exponential plus linear functions. The TT-OSL characteristics for sample YCW-4 are shown in Fig. 4, which contains the OSL decay curves and TT-OSL decay curves. The OSL signal is much larger than the TT-OSL signal (Fig. 4a). The growth curve for sample YCW-4 is shown in Fig. 4b. The TT-OSL characteristics of all samples were similar.

4.3.3. Results

The D_e values for samples in Yaochangwan section range from 256.8 ± 6.9 to 555.8 ± 22.5 Gy. These values increase with depth merely at the upper part of the loess section, but there is no distinct increase among the samples YCW-3, YCW-4, YCW-5, and even YCW-6. The total dose rate remained stable between 3.2 ± 0.2 and 3.5 ± 0.2 Gy/ka (Table 2). The age estimates appear to be in stratigraphic order only at the upper part of the Yaochangwan, ranging from 90.1 ± 9.1 ka to 172.6 ± 13.7 ka. But YCW-6 (154.7 ± 12.2 ka) at

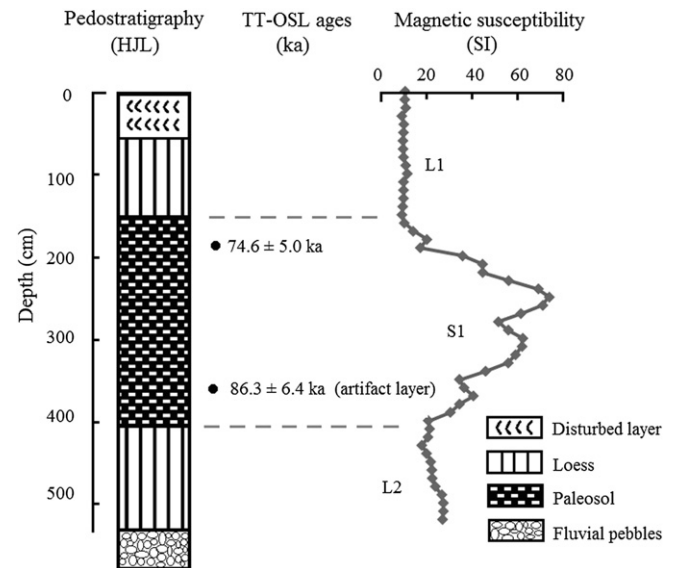


Fig. 5. Pedostratigraphy, TT-OSL ages, magnetic susceptibility of the Hejialiang loess section.

the bottom of the Yaochangwan section is even younger than YCW-4 (161.2 ± 11.2 ka) and YCW-5 (172.6 ± 13.7 ka). So the age of YCW-6 in artifact layer at the bottom of Yaochangwan section is questionable. Sample information and TT-OSL dating data for Hejialiang and Yaochangwan sections are listed in Table 2, and the TT-OSL age sequences are shown in Figs. 5 and 6. The typical OSL and TT-OSL growth curves of middle-sized quartz grains from the Yaochangwan Section show in Fig. 4. However, the dose response TT-OSL curves of the samples YCW-4, YCW-5, and YCW-6 did not show saturation tendency or saturation.

5. Discussion

The loess sequence in central Loess Plateau has been assigned a stratigraphic designation in consecutive order as follows: S0, L1, S1, L2, S2, L3, or S3... (Liu, 1985; Ding et al., 1992). The magnetic susceptibility record of Yaochangwan shows that this loess–paleosol sequence can be correlated with the Luochuan loess sequence on the Loess Plateau (Fig. 6). Therefore, it is possible to obtain age controls for the Yaochangwan loess sequence by consulting both the typical loess time series in the central Chinese Loess Plateau (Liu, 1985; Kukla et al., 1988; Lu et al., 1999, 2004) and the ice-volume time series of the North Hemisphere (Bassinot et al., 1994). However, there is a distinct shift in the magnetic susceptibility record below 720 cm in the Yaochangwan section. The reason for the abrupt shift may be explained that the magnetic susceptibility has a variable behavior with respect to different temperature–moisture environments. Ferromagnetic minerals are destroyed under high moisture (waterlogged), pedogenic conditions (Zhao et al., 2008). The abrupt shift of the magnetic susceptibility at 720 cm may reveal that the lower part of the section was deposited in a waterlogged environment while the upper part was not. But there is still a strong correlation between magnetic susceptibility of the Yaochangwan section and the typical loess–paleosol sequence (Fig. 6). When comparing these results with other loess–paleosol sections near this place, we found that there are almost identical structures and variations at the Qiaojayao and the Shangbaichuan loess sections (Lu et al., 2007, 2011; Wang et al., 2008a, 2008b), which are located in the Luonan Basin in the south marginal region of the Qinling Mountains.

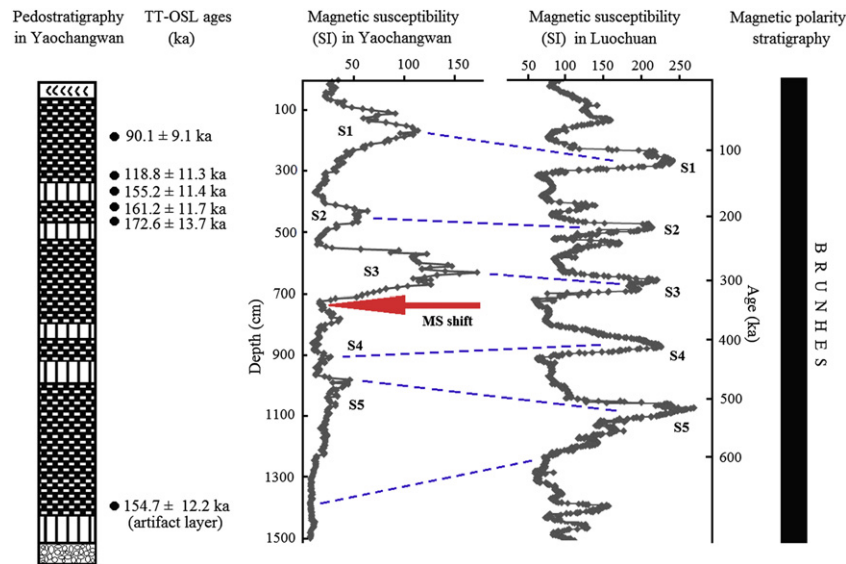


Fig. 6. Pedostratigraphy, TT-OSL ages, magnetic susceptibility and magnetostratigraphy of the Yaochangwan loess–paleosol sequence.

Mammalian fossil records were investigated in June 1980 (Tang and Zong, 1987), and all findings were from the loess-covered locality on the second terrace of Hanshui River. The mammalian fossil record also showed that aeolian loess covering the second Hanhui River terrace since the Middle Pleistocene (Tang and Zong, 1987).

The TT-OSL ages of HJL-1 (74.6 ± 5.0 ka) and HJL-2 (86.3 ± 6.4 ka) confirmed that the paleosol unit was deposited in the last interglacial period and can be correlated with S1 in Chinese Loess Plateau (Fig. 5). The TT-OSL ages of loess sediment at the upper part of the Yaochangwan section increase with depth. The two uppermost ages, 90.1 ± 9.1 ka and 118.8 ± 11.3 ka, confirmed that the first paleosol unit can be correlated with S1 paleosol. YCW-3 with an age of 155.2 ± 11.4 ka in the following loess unit shows that this unit can be correlated with the L2 loess. Then, the one-to-one correlation of the loess–paleosol alternations in the Yaochangwan and the Luochuan loess sections are established, and it is from S1 to L6 (Fig. 6).

The loess–paleosol deposit covered the second Hanhui River terrace since the middle Pleistocene. The TT-OSL age of YCW-6 (154.7 ± 12.2 ka) in depth 1400 cm of the bottom of Yaochangwan is questionable. The TT-OSL ages of YCW-1, YCW-2, YCW-3, and YCW-4 confirm the pedostratigraphy that S1, L2, and S2 exist in Yaochangwan section. However, the TT-OSL age of YCW-5 and YCW-6 conflict with the stratigraphic correlation. The dose response TT-OSL curves of YCW-4, YCW-5, and YCW-6 did not show saturation tendency or saturation (Fig. 4b), but D_e values did not increase any more. The ages for YCW-4, YCW-5, and YCW-6 should be thus underestimated. So, the TT-OSL method did not extend the age range beyond 180 ka in the Yaochangwan loess section. Therefore, the capability of the TT-OSL procedure extending the age range of loess deposits may be limited to the Hanzhong Basin, but this needs further investigation.

6. Conclusion

On the basis of TT-OSL ages for HJL-1 and HJL-2, the paleosol unit in the Hejialiang section corresponds to the S1 paleosol in Chinese Loess Plateau, and the age of artifact layer is 86.3 ± 6.4 ka. On the basis of the TT-OSL ages from YCW-1 to YCW-5 and the stratigraphy and magnetic susceptibility correlation with the typical Luochuan

loess–paleosol sequence, the first paleosol unit in the upper part of the Yaochangwan loess section corresponds to the S1 with an age of 71–129 ka (Lu et al., 1999), and the last paleosol unit at the bottom correlates to S5 soil with an age of 503–630 ka (Lu et al., 1999). The TT-OSL protocol may not extend the age range of loess sediments beyond 180 ka in Hanzhong Basin. Generally, the results suggest that hominids occupied at the Hejialiang site at approximately 100 ka ago; and, approximately 600 ka ago at the Yaochangwan and the Longgongsi sites.

Acknowledgments

We thank Thomas Stevens, Yongxiang Li, Wenchao Zhang, Kaifeng Yu, Haixin Zhuo, Chuanbin Yang for the help in field and laboratory. This Research is supported by the 100 Talents Program of Chinese Academy of Sciences (KZCX2-YW-BR-24), the National Natural Science Foundation of China (41072122 and 40901002) and the CAS Strategic Priority Research Program (No. XDA05130201).

Editorial handling by: R. Grun

Appendix A. Supplementary material

Supplementary material associated with this article can be found, in the online version, at doi:10.1016/j.quageo.2012.04.014.

References

- Aitken, M.J., Smith, B.W., 1988. Optical dating: recuperation after bleaching. *Quaternary Science Reviews* 7, 387–393.
- Adamic, G., Duller, G.A.T., Roberts, H.M., Wintle, A.G., 2010. Improving the TT-OSL SAR protocol through source trap characterisation. *Radiation Measurements* 45, 768–777.
- Bassinot, F.C., Labeyrie, L.D., Vincent, E., Quidelleur, X., Shackleton, N.J., Lancelot, Y., 1994. The astronomical theory of climate and the age of the Brunhes–Matuyama magnetic reversal. *Earth and Planetary Science Letters* 126, 91–108.
- Bøtter-Jensen, L., Mejdahl, V., Murray, A.S., 1999. New light on OSL. *Quaternary Science Reviews* 18, 303–309.
- Cande, S.C., Kent, D.V., 1995. Revised calibration of the geomagnetic polarity timescale for the Late Cretaceous and Cenozoic. *Journal of Geophysical Research* 100 (B4), 6093–6095.
- Ding, Z.L., Rutter, N., Han, J.M., Liu, T.S., 1992. A coupled environmental system formed at about 2.5 Ma in East-Asia. *Palaeogeography, Palaeoclimatology, Palaeoecology* 94, 223–242.
- Heller, F., Liu, T.S., 1984. Magnetism of Chinese loess deposits. *Geophysical Journal of the Royal Astronomical Society* 77, 125–141.

- Huang, W.W., Qi, G.Q., 1987. Preliminary observation of Liangshan Paleolithic site. *Acta Anthropologica Sinica* 6, 236–244 (in Chinese with English abstract).
- Kirschvink, J.L., 1980. The least-square line and plane and the analysis of aleo-magnetic data. *Geophysical Journal of the Royal Astronomical Society* 62, 699–718.
- Kukla, G., Heller, F., Liu, X.M., Xu, T.C., Liu, T.S., An, Z.S., 1988. Pleistocene climates in China dated by magnetic susceptibility. *Geology* 16, 811–814.
- Kukla, G., An, Z.S., 1989. Loess stratigraphy in central China. *Palaeogeography, Palaeoclimatology, Palaeoecology* 72, 203–225.
- Liu, T.S., 1985. Loess and the Environment. China Ocean Press, Beijing.
- Liu, T.S., Ding, Z.L., 1998. Chinese loess and the paleomonsoon. *Annual Review of Earth and Planetary Sciences* 26, 111–145.
- Lu, H.Y., Liu, X.D., Zhang, F.Q., An, Z.S., Dodson, J., 1999. Astronomical calibration of loess–paleosol deposits at Luochuan, central Chinese Loess Plateau. *Palaeogeography, Palaeoclimatology, Palaeoecology* 154, 237–246.
- Lu, H.Y., Zhang, F.Q., Liu, X.D., Duce, R., 2004. Periodicities of paleoclimatic variations recorded by the loesspaleosol sequences in China. *Quaternary Science Reviews* 23, 1891–1900.
- Lu, H.Y., Zhang, H.Y., Wang, S.J., Richard, C., Zhao, C.F., Thomas, S., Zhao, J., 2007. A preliminary survey on loess deposit in Eastern Qinling Mountains (central China) and its implication for estimating age of the Pleistocene lithic artifacts. *Quaternary Sciences* 27, 559–567 (in Chinese with English abstract).
- Lu, H.Y., Sun, X.F., Wang, S.J., Cosgrove, R., Zhang, H.Y., Yi, S.W., Ma, X.L., Wei, M., Yang, Z.Y., 2011. Ages for hominin occupation in Lushi Basin, middle of South Luo River, central China. *Journal of Human Evolution* 60, 612–617.
- Lu, N., Huang, W.W., Yin, S.P., Hou, Y.M., 2006. A new study on the Paleolithic materials from Liangshan site. *Acta Anthropologica Sinica* 25, 143–152 (in Chinese with English abstract).
- Lai, Z.P., Zoller, L., Fuchs, M., Bruckner, H., 2008. Alpha efficiency determination for OSL of quartz extracted from Chinese loess. *Radiation Measurements* 43, 767–770.
- Murray, A.S., Wintle, A.G., 2000. Luminescence dating of quartz using an improved single-aliquot regenerative-dose protocol. *Radiation Measurements* 32, 57–73.
- Porat, N., Duller, G.A.T., Roberts, H.M., Wintle, A.G., 2009. A simplified SAR protocol for TT-OSL. *Radiation Measurements* 44, 538–542.
- Prescott, J.R., Hutton, J.T., 1994. Cosmic ray contributions to dose rates for luminescence and ESR dating: large depths and long-term time variations. *Radiation Measurements* 23, 497–500.
- Rees-Jones, J., 1995. Optical dating of young sediments using fine-grain quartz. *Ancient TL* 13, 9–14.
- Smith, B.W., Aitken, M.J., Rhodes, E.J., Robinson, P.D., Geldard, D.M., 1986. Optical dating: methodological aspects. *Radiation Protection Dosimetry* 17, 229–233.
- Shaanxi Provincial Institute of Archaeology, Cultural Relics Administrative Committee of Shangluo District, Museum of Luonan County, 2007. *Huashilang (I): The Paleolithic Open-air Sites in the Luonan Basin, China*. Science Press, Beijing, pp. 1–250 (in Chinese with English abstract).
- Stevens, T., Buylaert, J.-P., Murray, A.S., 2009. Towards development of a broadly-applicable SAR TT-OSL dating protocol for quartz. *Radiation Measurements* 44, 639–645.
- Sun, X.F., Mercier, N., Falguères, C., Bahain, J.J., Despriée, J., Bayle, G., Lu, H.Y., 2010. Recuperated optically stimulated luminescence dating of middle-size quartz grains from the Paleolithic site of Bonneval (Eure-et-Loir, France). *Quaternary Geochronology* 5, 342–347.
- Tang, Y.J., Zong, G.F., 1987. On the new materials of Paleoliths from the Hanshui valley. *Acta Anthropologica Sinica* 6, 55–60 (in Chinese with English abstract).
- The Archaeological Team of Shaanxi Archaeological Institute, 1985. The discovery on Paleolithic at Longgangsi in Nanzheng County, Shaanxi. *Archaeology and Cultural Relics* 1, 1–12 (in Chinese with English abstract).
- The Archaeological Team of Shaanxi Archaeological Institute, 1988. The newly unearthed Paleolithic and Faunas at Longgangsi in Nanzheng, Shaanxi. *Prehistory Research*, 46–56 (in Chinese with English abstract).
- Tsukamoto, S., Duller, G.A.T., Wintle, A.G., 2008. Characteristics of thermally transferred optically stimulated luminescence (TT-OSL) in quartz and its potential for dating sediments. *Radiation Measurements* 43, 721–725.
- Wang, S.J., Cosgrove, R., Lu, H.Y., Shen, C., Wei, M., Zhang, X.B., 2008a. New progress on Paleolithic archaeological studies in the Luonan Basin, China. In: Kazuto, Matsufuji (Ed.), *Loess–paleosol and Paleolithic Chronology in East Asia*. Yuzankaku, Tokyo, pp. 145–161 (in Japanese with English abstract).
- Wang, S.J., Lu, H.Y., Zhang, H.Y., Zhao, J., Cosgrove, R., Yi, S.W., Sun, X.F., Wei, M., Garvey, J., Ma, X.L., 2008b. A preliminary survey of Paleolithic artifacts and loess deposition in the middle South Luo River, Eastern Qinling Mountains, central China. *Quaternary Sciences* 28, 988–999 (in Chinese with English abstract).
- Wang, X.L., Wintle, A.G., Lu, Y.C., 2006a. Thermally transferred luminescence in fine-grained quartz from Chinese loess: basic observations. *Radiation Measurements* 41, 649–658.
- Wang, X.L., Lu, Y.C., Wintle, A.G., 2006b. Recuperated OSL dating of fine-grained quartz in Chinese loess. *Quaternary Geochronology* 1, 89–100.
- Wang, X.L., Wintle, A.G., Lu, Y.C., 2007. Testing a single-aliquot protocol for recuperated OSL dating. *Radiation Measurements* 42, 380–391.
- Wang, Y.P., 2000. *Palaeolithic Archaeology in 20th Century China*. Cultural Relics Press, Beijing, pp. 1–262 (in Chinese).
- Wang, Y.P., 2008. *Roots of Pleistocene Hominids and Cultures in China*. Science Press, Beijing, pp. 1–340 (in Chinese).
- Yan, J.Q., 1981. Newly investigation of Liangshan Paleolithic in Hanzhong Basin, Shaanxi province. *Archaeology and Cultural Relics* 2, 1–5 (in Chinese).
- Yan, J.Q., 1980. The firstly discovery of Paleolithic artifacts at Longgangsi site in Hanzhong Basia, Shaanxi province. *Archaeology and Cultural Relics* 4, 1–5 (in Chinese).
- Zhao, J., Lu, H.Y., Wang, X.Y., Zhang, H.Y., Wang, S.J., 2008. Magnetic properties of the loess deposit in Eastern Qinling Mountains and an investigation on the magnetic susceptibility enhancement. *Acta Sedimentologica Sinica* 26, 58–68 (in Chinese with English abstract).